OPEN ACCESS
Journal of Innovative Optical Health Sciences
Vol. 15, No. 6 (2022) 2240007 (13 pages)

DOI: 10.1142/S1793545822400077

World Scientific
www.worldscientific.com

Photoswitchable semiconducting polymer dots with photosensitizer molecule and photochromic molecule loading for photodynamic cancer therapy

Lu Guo*, Bo Xu†, Haobin Chen‡ and Ying Tang*,§
*Department of Gastroenterology
The First Hospital of Jilin University
Changchun 130021, P. R. China

†Department of Urology
The First Hospital of Jilin University
Changchun 130021 P. R. China

‡Department of Biomedical Engineering
School of Basic Medical Sciences
Central South University, Changsha 410013, P. R. China
§tuboshu123@jlu.edu.cn

Received 21 May 2022
Revised 17 June 2022
Accepted 4 July 2022
Published 13 August 2022

Photodynamic therapy (PDT) is a new and rapidly developing treatment modality for clinical cancer therapy. Semiconductor polymer dots (Pdots) doped with photosensitizers have been successfully applied to PDT, and have made progress in the field of tumor therapy. However, the problems of severe photosensitivity and limited tissue penetration depth are needed to be solved during the implementation process of PDT. Here we developed the Pdots doped with photosensitizer molecule Chlorin e6 (Ce6) and photochromic molecule 1,2-bis(2,4-dimethyl-5-phenyl-3-thiophene)-3,3,4,5-hexafluoro-1-cyclopentene (BTE) to construct a photoswitchable nanoplatform for PDT. The Ce6-BTE-doped Pdots were in the green region, and the tissue penetration depth was increased compared with most Pdots in the blue region. The reversible conversion of BTE under different light irradiation was utilized to regulate the photodynamic effect and solve the problem of photosensitivity. The prepared Ce6-BTE-doped Pdots had small size, excellent optical property, efficient ROS generation and good photoswitchable ability. The cellular uptake, cytotoxicity, and photodynamic effect of the Pdots were detected in human colon tumor cells. The experiments *in vitro* indicated that Ce6-BTE-doped Pdots could exert excellent photodynamic effect in ON state and reduce photosensitivity in OFF state. These results demonstrated that this nanoplatform holds the potential to be used in clinical PDT.

Keywords: Photodynamic therapy; semiconductor polymer dots; photosensitizer; tumor therapy.

§Corresponding author.

1. Introduction

Photodynamic therapy (PDT) is a new type of cancer therapy. Essentially, the implementation process of PDT requires photosensitizers that selectively accumulate in tumor cells, light sources that specifically excite photosensitizers, and local irradiation of tumor tissues.[1–3] Under light source irradiation, the activated photosensitizer can transfer energy to oxygen molecules to produce cytotoxic reactive oxygen species (ROS) such as singlet oxygen ($^1O_2$), which could exhibit anti-tumor therapeutic effects.[4,5] In contrast with conventional cancer treatments, PDT possesses unique advantages including minimally invasive nature, tolerance of repeated doses, fast treatment process, and without additional damage to surrounding tissue.[6] At present, PDT has been applied in treatment of superficial bladder cancer, early and obstructive lung cancer, head and neck cancer, skin cancer and so on, and can also be used as adjuvant therapy after surgery to prevent tumor recurrence and metastasis. Although PDT has many unique advantages, it is limited in practical clinical applications due to poor solubility of photosensitizers, poor tumor selectivity and limited tissue penetration depth.[7,8] With the fast development of nanotechnology, researchers have developed a series of nanoparticles loaded with photosensitizers,[9] such as polymer nanoparticles,[10,11] upconversion nanoparticles,[12–14] gold nanoparticles,[15,16] mesoporous silica nanoparticles,[17–19] inorganic quantum dots[20,21] and so on, trying to solve the above problems related to photosensitizers.

Organic semiconductor polymers have been widely used in organic optoelectronic devices. They have excellent optical properties, such as larger optical absorption cross-section, higher fluorescence quantum efficiency and ultrafast radiative transition rate and so on, which are particularly suitable for the development of nanofluorescence techniques.[22] At present, hydrophobic organic semiconductor polymers can be prepared into water-soluble nanoparticles by nanoprecipitation method.[23] The mechanism of this method is to induce organic semiconductor polymers to fold into stable semiconductor polymer dots (Pdots) in water through the sudden changes of solvents. As a kind of nanomaterials, Pdots have many unique advantages for biomedical applications, including small size (5–30 nm), high brightness (fluorescence intensity of a Pdot is 100–10,000 times higher than that of a common fluorescent probe), low toxicity (non-toxic to cells at a dose of 1 mg/L), excellent water solubility, and without heavy metal components, thus attract great attention of researchers.[22] By loading functional molecules and modifying targeting molecules, Pdots have been applied in specific cell labeling,[24–26] *in vivo* fluorescence imaging,[27–31] photoacoustic imaging,[32,33] biosensing,[34,35] drug delivery,[36] and tumor therapy.[37] Currently, the Pdots doped with photosensitizers have also been successfully applied to PDT, and have made progress in the field of tumor therapy. Pdots can not only be served as a carrier to load hydrophobic photosensitizers, to solve the solubility problem of photosensitizers; Pdots can also be used as a matrix to absorb light and occur Förster resonance energy transfer (FRET) with the photosensitizers, thereby amplify ROS generation and kill tumor cells.[38]

In our previous researches, a variety of Pdots doped with photosensitizers were designed and constructed, and successfully applied to biological studies *in vivo* and *in vitro*.[39] Although Pdots doped with photosensitizers can effectively exert the photodynamic effect while implementing tumor fluorescence imaging, the following problems should be properly solved to achieve the clinical application: (1) Severe photosensitivity: most organic semiconductor polymers have a wide absorption spectrum, and can usually be excited by visible light. As a result, Pdots can easily be activated to produce ROS during non-treatment period, causing skin photosensitivity and damage to surrounding healthy tissues. (2) Limited tissue penetration depth: most Pdots are generally excited by visible light, while the chromophores of biological tissues can absorb light strongly in the visible spectrum, thus affect the imaging and therapeutic effects of Pdots in deep and solid tumors.

To solve the problems above, the semiconductor polymer Poly{[2,7-(9,9-bis-(2-octyl)-fluorene)]-alt-[5,5-(4,7-di-4-hexylthiophen-2-yl)benzo[c][1,2,5] thiadiazole)]} (PFDTBT) in the green region was selected to be served as a carrier and a light absorbing matrix, and its tissue penetration depth was increased compared with most semiconductor polymers in the blue region.[38] Subsequently, photosensitizer molecule Chlorin e6 (Ce6) and photochromic molecule 1,2-bis(2,4-dimethyl-5-phenyl-3-thiophene)-3,3,4,5-hexafluoro-1-cyclopentene (BTE) were doped

into PFDTBT to prepare Ce6-BTE-doped Pdots by nanoprecipitation method. BTE can exhibit strong absorption bands in the visible region and have effective quenching effect after ultraviolet-induced photocyclization (closed-ring form), which can convert to open-ring form and have no quenching effect under a different light irradiation.[40] Therefore, the reversible conversion of BTE under different light irradiation was utilized to regulate the photodynamic effect induced by Ce6-BTE-doped Pdots. This photoswitchable nanoplatform could exert the photodynamic effect in ON state and reduce the photosensitivity in OFF state, holding the potential to be applied in clinical PDT.

2. Experimental

2.1. *Material*

Chlorin e6 (Ce6), 1,2-bis(2,4-dimethyl-5-phenyl-3-thiophene)-3,3,4,5-hexafluoro-1-cyclopentene (BTE) were purchased from J&K Chemical Ltd. Poly(styrene-co-maleic anhydride) (PSMA), tetrahydrofuran (THF), 3-[4,5-dimethylthiazol-2-yl]-2,5-diphenyltetrazolium bromide (MTT), dimethyl sulfoxide (DMSO), 9,10-anthracenediyl-bis(methylene) dimalonic acid (ADMA) were purchased from Sigma-Aldrich. Lactate dehydrogenase (LDH) release assay kit was purchased from Beyotime biotechnology. Annexin V-FITC/PI apoptosis detection kit was purchased from KeyGEN technology. Cell culture medium, fetal bovine serum, penicillin/streptomycin and trypsin were purchased from Invitrogen.

2.2. *Preparation and characterization of Ce6-doped Pdots*

Synthetic steps of organic semiconductor polymer PFDTBT referred to the previous literature.[41] Ce6-doped Pdots were prepared by nanoprecipitation method. Semiconductor polymer PFDTBT, functional polymer PSMA and photosensitizer Ce6 were dissolved in anhydrous THF with a final concentration of 1 mg/mL as the original solution. Then 100 μL of PFDTBT, 30 μL of PSMA, 0–20 μL of Ce6 and a certain amount of THF were mixed to make 1 mL of the solution mixture. Subsequently, the solution mixture was quickly added to 10 mL of Milli Q water under sonication. After sonication for 1–2 min, the solution mixture was concentrated by nitrogen stripping under 100–120°. After that, the Ce6-doped Pdots solution was purified with a desalting column and filtered with a 0.22 μm filter. Then the emission spectra of Ce6-doped Pdots (the doping ratio of Ce6 was 0–20 wt.%) were detected by a fluorescence spectrometer (Hitachi F-4500) to explore the optimal doping ratio of Ce6. The particle size distribution, surface potential and morphology characteristics of Ce6-doped Pdots were detected by dynamic light scattering instrument (DLS, Malvern Zetasizer NanoZS), Zeta potentiometer and transmission electron microscope (TEM, Hitachi H-600), respectively.

2.3. *Preparation and characterization of Ce6-BTE-doped Pdots*

100 μL of PFDTBT, 30 μL of PSMA, the optimal doping ratio of Ce6, three times Ce6 concentration of BTE and a certain amount of THF were mixed to make 1 mL of the solution mixture. Then Ce6-BTE-doped Pdots were prepared by the method above. The particle size distribution, surface potential and morphology characteristics of Ce6-BTE-doped Pdots were detected by dynamic light scattering instrument, Zeta potentiometer and transmission electron microscope. In addition, to detect the stability of the Ce6-BTE-doped Pdots, absorption and emission spectra of Ce6-BTE-doped Pdots before and after 14 days storage at room temperature were detected by a spectrophotometer (Shimadzu UV-2550) and fluorescence spectrometer.

2.4. *Characterization of photoswitchable ability*

BTE was dissolved in anhydrous THF, and time-dependent absorption spectra of BTE under ultraviolet (UV) light irradiation (254 nm, 2 mW/cm^2) were detected by a spectrophotometer. When the absorption peak of BTE reached the maximum, the absorption spectra of BTE under green light irradiation (520 nm, 100 mW/cm^2) were detected. In the same way, the time-dependent absorption spectra and emission spectra of Ce6-BTE-doped Pdots under UV and green light irradiation were detected by a spectrophotometer and a fluorescence spectrometer. To detect the reversibility and reproducibility of photoswitching, the Ce6-BTE-doped Pdots were irradiated with repeated period of UV light (60 s) and green light (60 s) and its maximum emission peaks were detected.

2.5. *ROS detection*

ADMA solution (500 μg/mL) was prepared with PBS (pH = 7.4) and used as the original solution. First, ADMA solution (20 μg/ml) was irradiated with green light and its absorption spectra were detected by a spectrophotometer every 1 min. Then the Ce6-doped Pdots solution was mixed with the ADMA solution and diluted with PBS to make the Pdots concentration of 5 μg/mL, the ADMA concentration of 20 μg/mL. The solution mixture was irradiated with UV and green light, and the absorption spectra was detected every 1 min. Similarly, Ce6-BTE-doped Pdots and ADMA were mixed and diluted, and the absorption spectra of solution mixture under UV and green light irradiation were detected. Finally, the absorption values of ADMA at 259 nm were recorded every 1 min to detect the $^1O_2$ generation.

2.6. *Cell culture and fluorescence imaging*

HCT-116 cells (human colon tumor cells) were obtained from Cell Resource Center, Shanghai Academy of Life Sciences, Chinese Academy of Sciences. The cells were cultured at 37° in an incubator containing 5% CO_2. Cell culture medium contained 1640 basal culture medium, fetal bovine serum (10%) and penicillin/streptomycin (1%). When the confluence of cell growth reached 80%, cells were digested with 0.25% trypsin solution and collected by centrifugation (800 rpm, 5 min) for subsequent experiments.

For cellular imaging, 2×10^5 HCT-116 cells were placed into each well of 6-well plates for adherent culture. After culturing for 24 h, the cells of one group were incubated with 2–10 μg/mL of Ce6-BTE doped Pdots for 8 h. Then the cells were washed with PBS, and cell imaging was performed on a fluorescence microscope (Olympus IX71). Moreover, the cells of another group were incubated with 10 μg/ml of Ce6-BTE doped Pdots for 2–10 h.

2.7. *Cytotoxicity and photodynamic therapy in vitro*

Cytotoxicity and photodynamic effect were evaluated by MTT assay. Cytotoxicity of the Ce6-BTE-doped Pdots without light irradiation was investigated before *in vitro* PDT study. HCT-116 cells were collected, and 1×10^4 cells were seeded to each well of 96-well plates. After 24 h, the cells were incubated with 0–100 μg/mL Ce6-BTE-doped Pdots for 24 h and the conventional process of MTT assay was carried out. MTT assay was measured by a microplate reader (BioTek Cytation3).

MTT assay was also used to detect the photodynamic effect *in vitro*. 1×10^4 cells were seeded to each well of 96-well plates and routinely cultured. The HCT-116 cells were incubated with 10 μg/mL of Ce6-doped Pdots and Ce6-BTE-doped Pdots for 8 h. After 8 h, the 96-well plates were respectively irradiated with UV light (0–9 min) and green light (0–15 min), and then were incubated for 16 h. Next, the conventional process of MTT assay was carried out.

LDH release assay was also carried out to evaluate the photodynamic effect. 1×10^4 cells were seeded to each well of 96-well plates and routinely cultured. The HCT-116 cells were incubated with 2–10 μg/mL of Ce6-doped Pdots and Ce6-BTE-doped Pdots for 8 h. After 8 h, the 96-well plates were respectively irradiated with UV light (5 min) and green light (15 min), and then were incubated for 16 h. Next, the LDH release was detected by the LDH release assay kit.

Furthermore, Annexin V-FITC/PI staining was used to detect the photodynamic effect more accurately. 2×10^5 cells were seeded to each well of 6-well plates and routinely cultured. The HCT-116 cells were incubated with 2–8 μg/mL of Ce6-BTE-doped Pdots for 8 h and irradiated with green light for 15 min, and then were incubated for 16 h. Finally, the cells were collected and stained with Annexin V-FITC/PI apoptosis detection kit for flow cytometry (BD FACS Calibur, BD Accuri C6).

3. Results and Discussion

3.1. *Preparation and characterization of Ce6-doped Pdots*

The synthesis of the organic semiconductor polymer PFDTBT referred to the previous literature.[41] Since the absorption spectrum of PFDTBT was in the green region, the tissue penetration depth was increased compared with most semiconductor polymers in the blue region. As we all know, Ce6 is a photosensitizer with excellent properties including a large absorption coefficient in the infrared region, a strong photodynamic response ability, and little

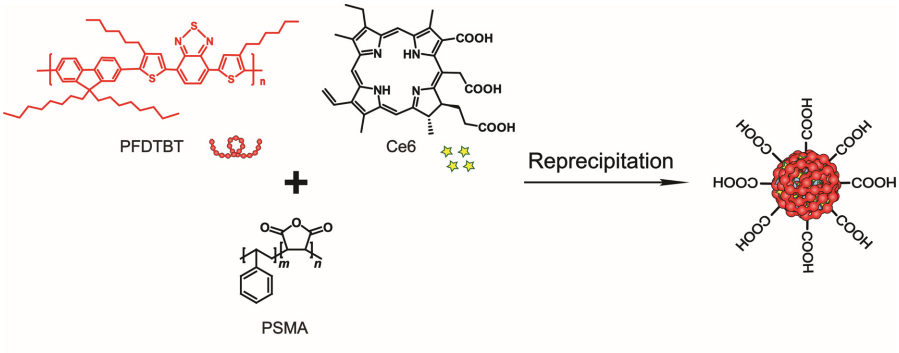

Scheme 1. Preparation of Ce6-doped Pdots.

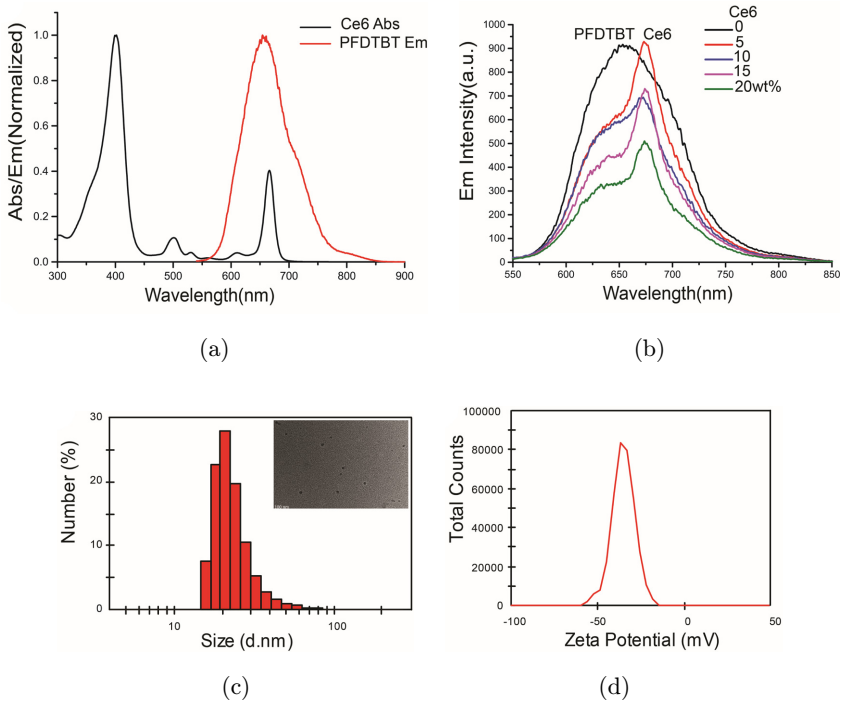

Fig. 1. Preparation and characterization of Ce6-doped Pdots. (a) Emission spectra of polymer PFDTBT and absorption spectra of photosensitizer Ce6. (b) Emission spectra of Pdots doped with different ratios of Ce6. (c) Particle size distribution and TEM image of Ce6-doped Pdots. (d) Zeta potential of Ce6-doped Pdots.

toxic side effects.[42] However, Ce6 is an amphiphilic compound with poor solubility in aqueous solution, limiting its clinical application. Therefore, we planned to establish a nanoplatform based on Pdots, which can not only be used as a carrier for Ce6 to solve the solubility problem, but also served as a light absorbing matrix to occur FRET with Ce6 for amplifying ROS generation and killing tumor cells (Scheme 1).

Figure 1(a) shows the spectral overlap between the polymer PFDTBT and the photosensitizer Ce6, indicating the possibility of FRET occurring, which was a requirement for amplifying the generation of ROS. Figure 1(b) shows the emission spectra of Pdots doped with different ratios of Ce6. With the increase of doping ratio (0–20 wt.%), the emission peak of Ce6 increased initially and then decreased. When the doping ratio was 5%, the emission peak value of Ce6 reached the maximum, indicating the efficiency of FRET between PFDTBT and Ce6 was the highest, therefore the optimal doping ratio of Ce6 was set as 5%. Subsequently, the particle size distribution, surface potential and morphological feature of Ce6-doped Pdots were detected. In Fig. 1(c), the particle size distribution of Ce6-doped Pdots was 20–30 nm. Transmission electron microscopy image

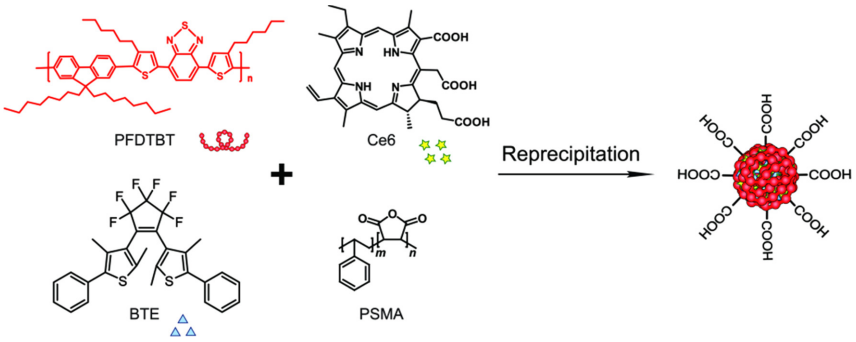

(a)

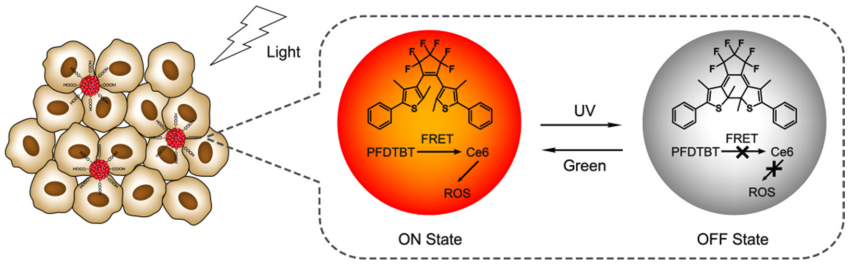

(b)

Scheme 2. Preparation and photodynamic effect of Ce6-BTE-doped Pdots.

showed that Ce6-doped Pdots were distributed evenly with uniform size, and these Pdots were suitable for the following biological experiments. Figure 1(d) shows that the Zeta potential of Ce6-doped Pdots was −35.5 mV, which was consistent with the basic characteristics of Pdots.

3.2. *Preparation and characterization of Ce6-BTE-doped Pdots*

As a photochromic molecule, BTE is essentially a diarylethene, which has many advantages of good thermal stability, strong fatigue resistance, fast response time, and high quantum yield. Based on these excellent properties, BTE has been used as a quencher for various fluorescent nanoparticles. BTE generally has no quenching effect in the open-ring form, however, when irradiated with UV light, the open-ring form can convert to the closed-ring form through photocyclization. The closed-ring form of BTE has a high absorption peak in the visible region, which can effectively quench the fluorescence emitted from most fluorophores. Nevertheless, when BTE is irradiated with a different light, it returns to the open-ring form and no longer has the quenching effect. Therefore, we planned to utilize the reversible conversion of BTE under different light irradiation to obtain the photoswitchable Pdots, trying to solve the problem of photosensitivity in PDT. As shown in Scheme 2, Ce6-BTE-doped Pdots were prepared by nanoprecipitation with Ce6 and BTE loading simultaneously according to a certain ratio. In this nanoplatform, when irradiated with UV light, BTE was a closed-ring form and the absorption peak increased in the visible region, which could not only interfere the FRET between PFDTBT and Ce6, but also quench the fluorescence of Ce6, thereby Ce6-BTE-doped Pdots could not exert the photodynamic effect (OFF state). On the contrary, when irradiated with green light, BTE converted to an open-ring form and the absorption peak decreased, which did not affect the FRET and the fluorescence of Ce6, thus Ce6-BTE-doped Pdots could exert the photodynamic effect (ON state).[40]

Figure S1(a) shows the absorption spectra changes of BTE under UV light irradiation. With the extension of irradiation time, the absorption peak of BTE in the visible region gradually increased and reached the maximum when irradiated for 90 s. Figure S1(b) shows the absorption spectra changes of BTE under green light irradiation after exposed to UV light. The absorption peak of BTE gradually decreased with the extension of irradiation time, when irradiated with green light for 120 s,

the absorption peak of BTE almost returned to the baseline. These experiments showed that BTE possessed the ability to convert between the two forms sensitively and flexibly, which was the basis for the construction of photoswitchable Pdots. Figures 2(a) and 2(b) show the absorption spectra of Ce6-BTE-doped Pdots under UV and green light irradiation, respectively, and there was no significant change in the absorption spectra. Furthermore, the emission spectra changes of Ce6-BTE-doped Pdots under UV light irradiation were shown in Fig. 2(c), indicating that with the extension of irradiation time, the emission peak of Ce6-BTE-doped Pdots gradually decreased and reached the minimum after irradiation for 75 s. However, when Ce6-BTE-doped Pdots were irradiated with green light after exposed to UV light, the emission peak of Ce6-BTE-doped Pdots gradually recovered with the extension of irradiation time (Fig. 2(d)). The experimental results above indicated that Ce6-BTE-doped Pdots could be switched easily between ON/OFF state under UV and green light irradiation, making it possible to establish the photoswitchable nanoplatform. In order to further detect the cyclic photoconversion of Ce6-BTE-doped Pdots, they were irradiated with UV and green light circularly. As shown in Fig. S2, the Ce6-BTE-doped Pdots were switched reversibly between ON/OFF state for five cycles, indicating the good fatigue resistance. Figures 2(e) and 2(f) show that Ce6-BTE-doped Pdots were distributed uniformly, their particle size distribution was 20–30 nm and Zeta potential was −32.8 mV. Moreover, the spectroscopy of Ce6-BTE-doped Pdots after 14 days storage was compared with before to check the colloidal stability. The results showed that there was no significant change in the absorption and emission spectra after 14 days storage, confirming

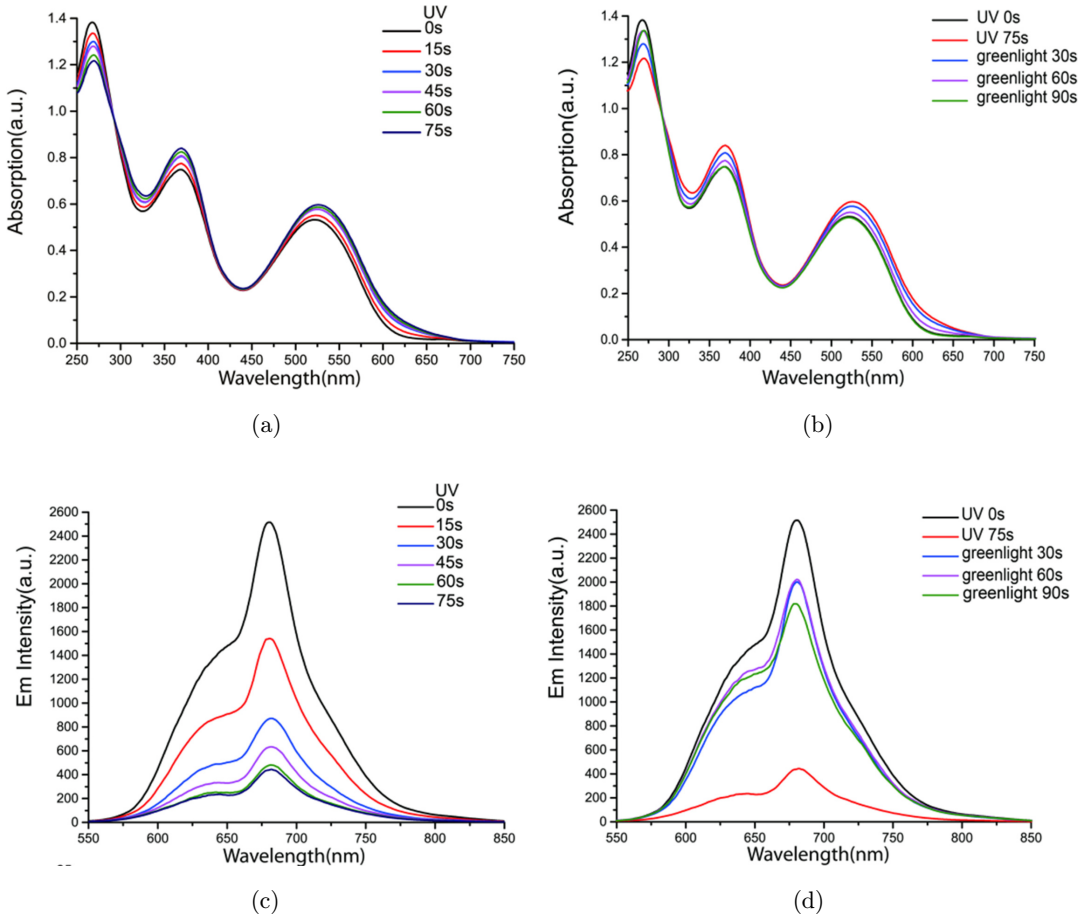

Fig. 2. Preparation and characterization of Ce6-BTE-doped Pdots. Absorption spectra (a) and emission spectra (c) of Ce6-BTE-doped Pdots under UV irradiation. Absorption spectra (b) and emission spectra (d) of Ce6-BTE-doped Pdots under green light irradiation after exposed to UV. (e) Particle size distribution and TEM image of Ce6-BTE-doped Pdots. (f) Zeta potential of Ce6-BTE-doped Pdots.

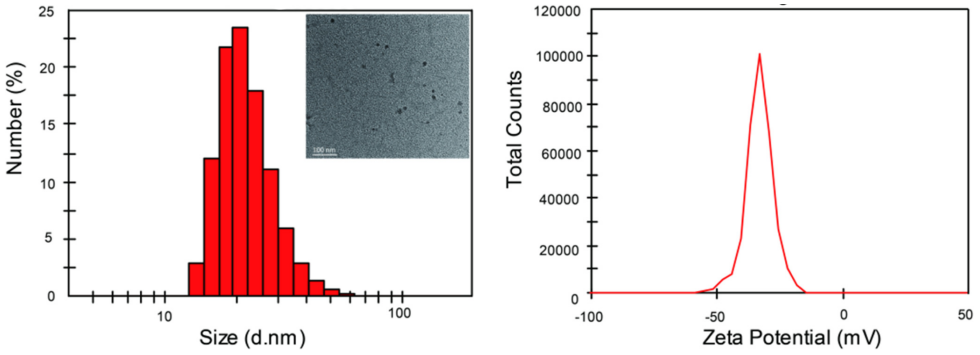

(e) (f)

Fig. 2. (*Continued*)

the good stability of Ce6-BTE-doped Pdots (Fig. S3).

3.3. *ROS detection*

$^1O_2$ is the main cytotoxic substance of type II photochemical reaction in PDT, which can kill tumor cells and destroy tumor tissues.[4] Therefore, detection of $^1O_2$ generation plays an important role in evaluating the therapeutic effect of PDT. In this experiment, we selected ADMA as a probe to detect the $^1O_2$ generation of Pdots. Since $^1O_2$ can induce photodegradation of ADMA, the absorption value changes at 259 nm of ADMA can be used to calculate the $^1O_2$ yield. First, the absorption spectra of ADMA alone under light irradiation were measured, to exclude the possibility of photodegradation induced by light irradiation. As shown in Fig. 3(a), there was no significant change in the absorption spectra of ADMA, indicating that only green light irradiation did not cause ADMA photodegradation. Figures 3(b) and 3(d) show that Ce6-doped Pdots and Ce6-BTE-doped Pdots induced significant photodegradation of ADMA under green light irradiation, indicating that Ce6-BTE-doped Pdots could produce abundant $^1O_2$ in ON state and was comparable to Ce6-doped Pdots. Figures 3(c) and 3(e) show the absorption spectra changes of ADMA, when Ce6-doped Pdots and Ce6-BTE-doped Pdots mixed with ADMA were irradiated with UV light. The results indicated that Ce6-doped Pdots produced a small amount of $^1O_2$, whereas Ce6-BTE-doped Pdots did not produce $^1O_2$ in OFF state. Subsequently, in order to display the $^1O_2$ generation more intuitively, a statistical analysis of the ADMA absorption value at 259 nm was carried out (Fig. 3(f)). The experimental results demonstrated that Ce6-BTE-doped Pdots possessed the ability to produce a large amount of ROS in ON state, which was comparable to Ce6-doped Pdots and promising for photodynamic cancer therapy. Moreover, the $^1O_2$ yield of Ce6-BTE-doped Pdots in OFF state was significantly lower than that of Ce6-doped Pdots, which was helpful to reduce the photosensitivity during PDT.

3.4. *Cell fluorescence imaging*

Cellular uptake of Pdots is necessary for exerting photodynamic effect. Since Pdots have excellent fluorescence property, it becomes easier to monitor the uptake of Pdots by tumor cells. We designed dose-dependent and time-dependent experiments to evaluate the cellular uptake efficiency of Ce6-BTE-doped Pdots. As shown in Fig. 4(a), tumor cells were incubated with different doses of Ce6-BTE-doped Pdots, and the intracellular red fluorescence gradually enhanced with the increase of incubation dose, indicating the cellular uptake was dose-dependent. With the incubation dose of 10 ug/ml, the fluorescence intensity in tumor cells reached the maximum. Figure 4(b) shows the time-dependent fluorescence imaging of tumor cells incubated with Ce6-BTE-doped Pdots. Intracellular red fluorescence was gradually enhanced with increasing the incubation time, and the fluorescence intensity reached the maximum with the incubation time for 8–10 h. The results above demonstrated that the cellular uptake of Ce6-BTE-doped Pdots was dose-dependent and time-dependent, and effective

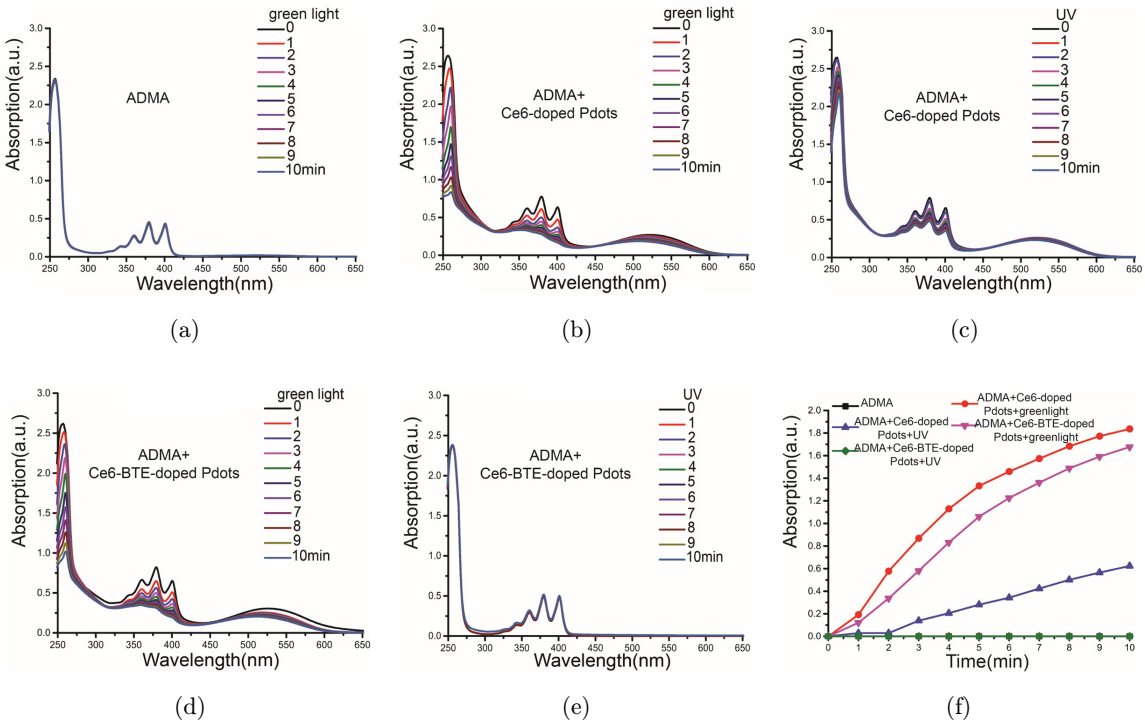

Fig. 3. ROS detection. (a) Absorption spectra of ADMA alone under green light irradiation. Absorption spectra of ADMA mixed with Ce6-doped Pdots under green light irradiation (b) and UV irradiation (c). Absorption spectra of ADMA mixed with Ce6-BTE-doped Pdots under green light irradiation (d) and UV irradiation (e). (f) Absorption value changes of ADMA at 259 nm.

cellular uptake was achieved with relatively low incubation dose and short incubation time.

3.5. *Cytotoxicity and photodynamic therapy in vitro*

Cytotoxicity is an important factor for evaluating the biocompatibility of Pdots. MTT assay was carried out to detect the cytotoxicity of Ce6-BTE-doped Pdots. In Fig. 5(a), tumor cells were incubated with 0–100 ug/ml Ce6-BTE-doped Pdots for 24 h, and the Ce6-BTE-doped Pdots exhibited negligible cytotoxicity. Meanwhile, MTT assay was also used to detect the photodynamic effect *in vitro*. As shown in Fig. 5(b), tumor cells were, respectively, incubated with Ce6-BTE-doped Pdots and

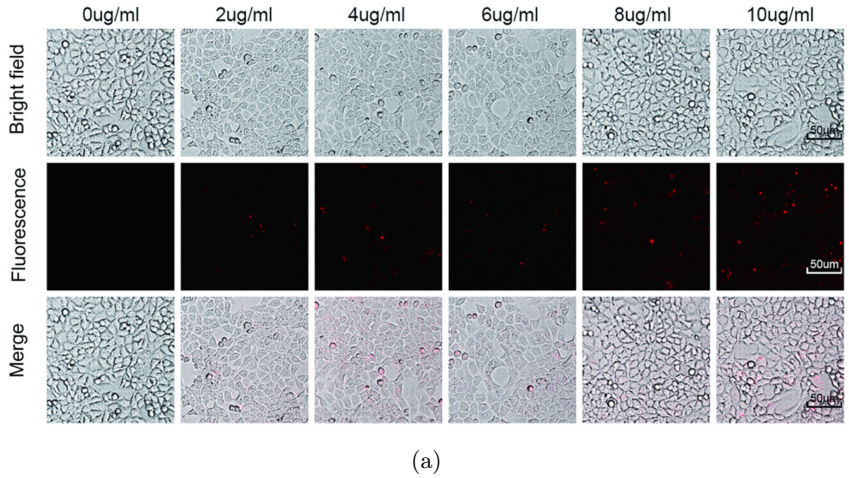

Fig. 4. Cell fluorescence imaging. (a) Dose-dependent cell fluorescence imaging of Ce6-BTE-doped Pdots. (b) Time-dependent cell fluorescence imaging of Ce6-BTE-doped Pdots.

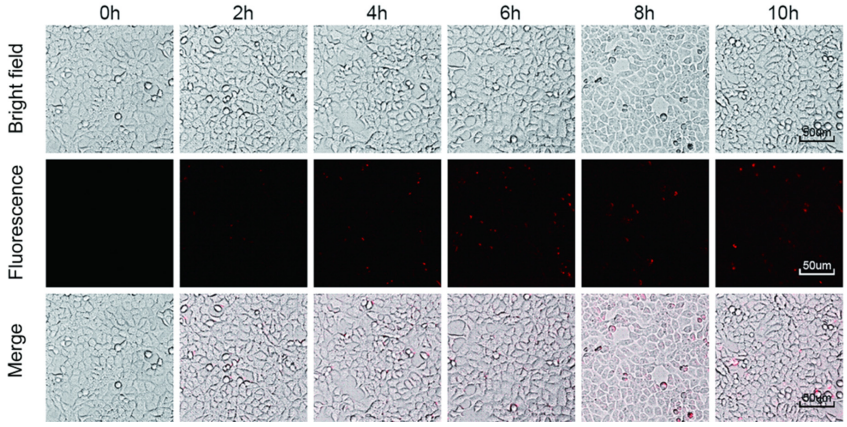

(b)

Fig. 4. (*Continued*)

Ce6-doped Pdots, and the cell viability apparently decreased with the extension of green light irradiation time. When tumor cells were incubated with 10 μg/mL Ce6-BTE-doped Pdots and irradiated with green light for 15 min, the cell viability (%) reduced to 30–40%, which displayed the excellent photodynamic effect in ON state and was comparable to Ce6-doped Pdots. In Fig. 5(c), with the

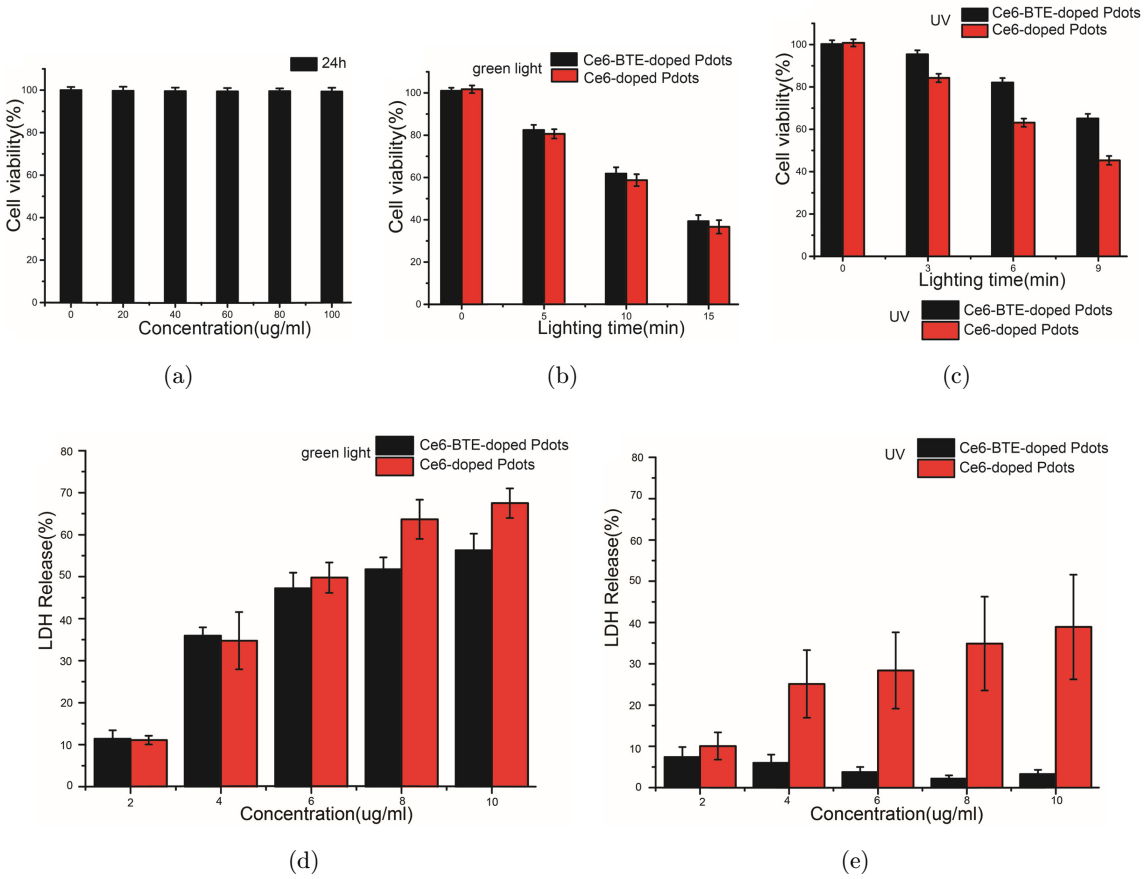

(a) (b) (c)

(d) (e)

Fig. 5. Cytotoxicity and *in vitro* photodynamic effect. (a) Cell viability of tumor cells incubated with 0–100 ug/mL Ce6-BTE-doped Pdots for 24 h. Cell viability of tumor cells incubated with Ce6-BTE-doped Pdots and Ce6-doped Pdots under green light irradiation (b) and UV irradiation (c). LDH release of tumor cells incubated with Ce6-BTE-doped Pdots and Ce6-doped Pdots under green light irradiation (d) and UV irradiation (e).

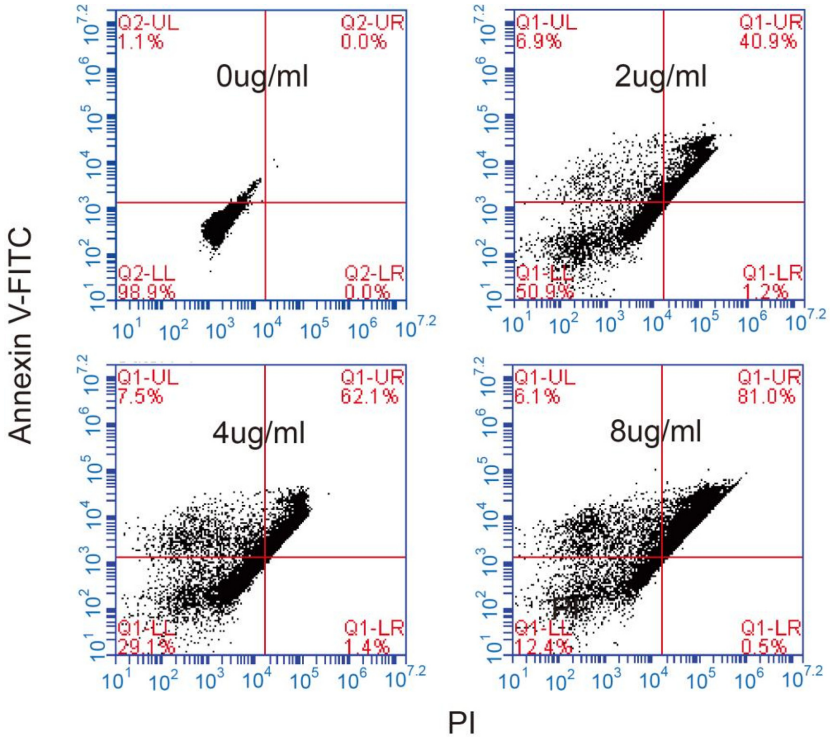

Fig. 6. Annexin V-FITC/PI staining of tumor cells incubated with Ce6-BTE-doped Pdots and irradiated with green light.

extension of UV light irradiation time, Ce6-doped Pdots exhibited more severe toxicity than Ce6-BTE-doped Pdots, indicating that Ce6-BTE-doped Pdots could reduce the photosensitivity in OFF state.

Subsequently, LDH release experiment was used to evaluate the photodynamic effect *in vitro*. Cell membrane damages caused by apoptosis or necrosis generally lead to the release of enzymes, including LDH, which is widely used to evaluate cell membrane integrity and cell damage. For Fig. 5(d), tumor cells were respectively incubated with Ce6-BTE-doped Pdots and Ce6-doped Pdots and irradiated with green light. With the increase of incubation dose, the LDH release (%) increased significantly, indicating that both of the two kinds of Pdots could effectively kill tumor cells. As shown in Fig. 5(e), the LDH release (%) caused by Ce6-BTE-doped Pdots under UV light irradiation was significantly lower than that of Ce6-doped Pdots, indicating Ce6-BTE-doped Pdots did not exert obvious photodynamic effect in OFF state.

Furthermore, Annexin V-FITC/PI staining is usually used to detect cell apoptosis or necrosis. Thus, we carried out Annexin V-FITC/PI staining to evaluate the photodynamic effect of Pdots (Fig. 6). Tumor cells were incubated with Ce6-BTE-doped Pdots and irradiated with green light, and the percentage of late apoptosis or necrosis gradually increased with the increase of incubation dose. When the incubation dose was 8 ug/ml, the percentage of late apoptosis or necrosis reached 81%, indicating that Ce6-BTE-doped Pdots had a good photodynamic effect in ON state.

4. Conclusion

Photodynamic therapy has achieved rapid development due to its unique advantages, but the problems of severe photosensitivity and limited tissue penetration depth limit the clinical application of photodynamic therapy. This study used a semiconductor polymer PFDTBT in the green region that has increased tissue penetration depth to construct a nanoplatform with photoswitchable properties, and *in vitro* experiments proved that the nano-platform has a great photodynamic therapy effect and excellent photoswitchable properties, which is conducive to reducing phototoxicity of photodynamic therapy and beneficial to the practical clinical application of photodynamic therapy. Outside of this nanoplatform, our research group plans to explore more sensitive and stable photodynamic therapeutic nanoplatforms with

photoswitchable properties, and the performance of the nanoplatforms *in vivo* experiments.

Conflicts of Interest

There are no conflicts to declare.

Acknowledgments

This work was supported by the science and technology research project of education department of Jilin province (JJKH20211189KJ) and Jilin province medical and health talents special project.

References

1. D. E. Dolmans, D. Fukumura, R. K. Jain, "Photodynamic therapy for cancer," *Nat. Rev. Cancer.* **3**, 380–387 (2003).
2. M. Triesscheijn, P. Baas, J. H. Schellens, F. A. Stewart, "Photodynamic therapy in oncology," *Oncologist* **11**, 1034–1044 (2006).
3. N. M. Idris, M. K. Gnanasammandhan, J. Zhang, P. C. Ho, R. Mahendran, Y. Zhang, "In vivo photodynamic therapy using upconversion nanoparticles as remote-controlled nanotransducers," *Nat. Med.* **18**, 1580–1585 (2012).
4. M. Ethirajan, Y. Chen, P. Joshi, R. K. Pandey, "The role of porphyrin chemistry in tumor imaging and photodynamic therapy," *Chem. Soc. Rev.* **40**, 340–362 (2011).
5. M. Niedre, M. S. Patterson, B. C. Wilson, "Direct near-infrared luminescence detection of singlet oxygen generated by photodynamic therapy in cells in vitro and tissues in vivo," *Photochem. Photobiol.* **75**, 382–391 (2002).
6. J. F. Lovell, T. W. B. Liu, J. Chen, G. Zheng, "Activatable photosensitizers for imaging and therapy," *Chem. Rev.* **110**, 2839–2857 (2010).
7. S. Cui, D. Yin, Y. Chen, Y. Di, H. Chen, Y. Ma, S. Achilefu, Y. Gu, "In vivo targeted deep-tissue photodynamic therapy based on near-infrared light triggered upconversion nanoconstruct," *ACS Nano* **7**, 676–688 (2013).
8. W. Fan, P. Huang, X. Chen, "Overcoming the Achilles' heel of photodynamic therapy," *Chem. Soc. Rev.* **45**, 6488–6519 (2016).
9. S. S. Lucky, K. C. Soo, Y. Zhang, "Nanoparticles in photodynamic therapy," *Chem. Rev.* **115**, 1990–2042 (2015).
10. M. Rojnik, P. Kocbek, F. Moret, C. Compagnin, L. Celotti, M. J. Bovis, J. H. Woodhams, A. J. MacRobert, D. Scheglmann, W. Helfrich, M. J. Verkaik, E. Papini, E. Reddi, J. Kos, "In vitro and in vivo characterization of temoporfin-loaded PEGylated PLGA nanoparticles for use in photodynamic therapy," *Nanomedicine* **7**, 663–677 (2012).
11. W. S. Chenggen Qian, J. Yu, Y. Chen, Q. Hu, X. Xiao, "Light-activated hypoxia-responsive nanocarriers for enhanced anticancer therapy," *Adv. Mater.* **28**, 3313–3320 (2016).
12. K. Liu, X. Liu, Q. Zeng, Y. Zhang, L. Tu, T. Liu, X. Kong, Y. Wang, F. Cao, S. A. G. Lambrechts, M. C. G. Aalders, H. Zhang, "Covalently assembled NIR nanoplatform for simultaneous fluorescence imaging and photodynamic therapy of cancer cells," *ACS Nano* **6**, 4054–4062 (2012).
13. M. Wang, Z. Chen, W. Zheng, H. Zhu, S. Lu, E. Ma, D. Tu, S. Zhou, M. Huang, X. Chen, "Lanthanide-doped upconversion nanoparticles electrostatically coupled with photosensitizers for near-infrared-triggered photodynamic therapy," *Nanoscale* **6**, 8274–8282 (2014).
14. G. Tian, Z. Gu, L. Zhou, W. Yin, X. Liu, L. Yan, S. Jin, W. Ren, G. Xing, S. Li, Y. Zhao, "Mn 2+ dopant-controlled synthesis of NaYF 4:Yb/Er upconversion nanoparticles for in vivo imaging and drug delivery," *Adv. Mater.* **24**, 1226–1231 (2012).
15. B. Jang, J. Y. Park, C. H. Tung, I. H. Kim, Y. Choi, "Gold nanorod-photosensitizer complex for near-infrared fluorescence imaging and photodynamic/photothermal therapy in vivo," *ACS Nano* **5**, 1086–1094 (2011).
16. L. Gao, J. Fei, J. Zhao, H. Li, Y. Cui, J. Li, "Hypocrellin-loaded gold nanocages with high two-photon efficiency for photothermal/photodynamic cancer therapy in vitro," *ACS Nano* **6**, 8030–8040 (2012).
17. J. Qian, A. Gharibi, S. He, "Colloidal mesoporous silica nanoparticles with protoporphyrin IX encapsulated for photodynamic therapy," *J. Biomed. Opt.* **14**, 014012 (2009).
18. I. T. Teng, Y. J. Chang, L. S. Wang, H. Y. Lu, L. C. Wu, C. M. Yang, C. C. Chiu, C. H. Yang, S. L. Hsu, J. A. Ho, "Phospholipid-functionalized mesoporous silica nanocarriers for selective photodynamic therapy of cancer," *Biomaterials* **34**, 7462–7470 (2013).
19. Z. X. Zhao, Y. Z. Huang, S. G. Shi, S. H. Tang, D. H. Li, X. L. Chen, "Cancer therapy improvement with mesoporous silica nanoparticles combining photodynamic and photothermal therapy," *Nanotechnology* **25**, 285701 (2014).
20. L. Shi, B. Hernandez, M. Selke, "Singlet oxygen generation from water-soluble quantum dot-organic

dye nanocomposites," *J. Am. Chem. Soc.* **128**, 6278–6279 (2006).
21. J. M. Tsay, M. Trzoss, L. Shi, X. Kong, M. Selke, M. E. Jung, S. Weiss, "Singlet oxygen production by peptide-coated quantum dot-photosensitizer conjugates," *J. Am. Chem. Soc.* **129**, 6865–6871 (2007).
22. C. Wu, D. T. Chiu, "Highly fluorescent semiconducting polymer dots for biology and medicine," *Angew. Chem. Int. Ed.* **52**, 3086–3109 (2013).
23. J. Pecher, S. Mecking, "Nanoparticles of conjugated polymers," *Chem. Rev.* **110**, 6260–6279 (2010).
24. C. Wu, Y. Jin, T. Schneider, D. R. Burnham, P. B. Smith, D. T. Chiu, "Ultrabright and bioorthogonal labeling of cellular targets using semiconducting polymer dots and click chemistry," *Angew. Chem., Int. Ed.* **49**, 9436–9440 (2010).
25. C. Wu, T. Schneider, M. Zeigler, J. Yu, P. G. Schiro, D. R. Burnham, J. D. McNeill, D. T. Chiu, "Bioconjugation of ultrabright semiconducting polymer dots for specific cellular targeting," *J. Am. Chem. Soc.* **132**, 15410–15417 (2010).
26. F. Ye, C. Wu, Y. Jin, M. Wang, Y. H. Chan, J. Yu, W. Sun, S. Hayden, D. T. Chiu, "A compact and highly fluorescent orange-emitting polymer dot for specific subcellular imaging," *Chem. Commun.* **48**, 1778–1780 (2012).
27. S. Kim, C. K. Lim, J. Na, Y. D. Lee, K. Kim, K. Choi, J. F. Leary, I. C. Kwon, "Conjugated polymer nanoparticles for biomedical in vivo imaging," *Chem. Commun.* **46**, 1617–1619 (2010).
28. C. Wu, S. J. Hansen, Q. Hou, J. Yu, M. Zeigler, Y. Jin, D. R. Burnham, J. D. McNeill, J. M. Olson, D. T. Chiu, "Design of highly emissive polymer dot bioconjugates for in vivo tumor targeting," *Angew. Chem. Int. Ed.* **50**, 3430–3434 (2011).
29. K. Pu, N. Chattopadhyay, J. Rao, "Recent advances of semiconducting polymer nanoparticles in in vivo molecular imaging," *J. Control. Release* **240**, 312–322 (2016).
30. H. Zhu, Y. Fang, X. Zhen, N. Wei, Y. Gao, K. Q. Luo, C. Xu, H. Duan, D. Ding, P. Chen, K. Pu, "Multilayered semiconducting polymer nanoparticles with enhanced NIR fluorescence for molecular imaging in cells, zebrafish and mice," *Chem. Sci.* **7**, 5118–5125 (2016).
31. X. Zhen, C. Zhang, C. Xie, Q. Miao, K. L. Lim, K. Pu, "Intraparticle energy level alignment of semiconducting polymer nanoparticles to amplify chemiluminescence for ultrasensitive in vivo imaging of reactive oxygen species," *ACS Nano.* **10**, 6400–6409 (2016).
32. Q. Miao, Y. Lyu, D. Ding, K. Pu, "Semiconducting oligomer nanoparticles as an activatable photoacoustic probe with amplified brightness for in vivo imaging of pH," *Adv. Mater.* **28**, 3662–3668 (2016).
33. Y. Lyu, Y. Fang, Q. Miao, X. Zhen, D. Ding, K. Pu, "Intraparticle molecular orbital engineering of semiconducting polymer nanoparticles as amplified theranostics for in vivo photoacoustic imaging and photothermal therapy," *ACS Nano* **10**, 4472–4481 (2016).
34. Y. H. Chan, C. Wu, F. Ye, Y. Jin, P. B. Smith, D. T. Chiu, "Development of ultrabright semiconducting polymer dots for ratiometric pH sensing," *Anal. Chem.* **83**, 1448–1455 (2011).
35. F. Ye, C. Wu, Y. Jin, Y. H. Chan, X. Zhang, D. T. Chiu, "Ratiometric temperature sensing with semiconducting polymer dots," *J. Am. Chem. Soc.* **133**, 8146–8149 (2011).
36. J. H. Moon, E. Mendez, Y. Kim, A. Kaur, "Conjugated polymer nanoparticles for small interfering RNA delivery," *Chem. Commun.* **47**, 8370–8372 (2011).
37. Y. Lyu, C. Xie, S. A. Chechetka, E. Miyako, K. Pu, "Semiconducting polymer nanobioconjugates for targeted photothermal activation of neurons," *J. Am. Chem. Soc.* **138**, 9049–9052 (2016).
38. S. Li, K. Chang, K. Sun, Y. Tang, N. Cui, Y. Wang, W. Qin, H. Xu, C. Wu, "Amplified singlet oxygen generation in semiconductor polymer dots for photodynamic cancer therapy," *ACS Appl. Mater. Interfaces* **8**, 3624–3634 (2016).
39. Y. Tang, H. Chen, K. Chang, Z. Liu, Y. Wang, S. Qu, H. Xu, C. Wu, "Photo-cross-linkable polymer dots with stable sensitizer loading and amplified singlet oxygen generation for photodynamic therapy," *ACS Appl. Mater. Interfaces* **9**, 3419–3431 (2017).
40. C. T. Kuo, A. M. Thompson, M. E. Gallina, F. Ye, E. S. Johnson, W. Sun, M. Zhao, J. Yu, I. C. Wu, B. Fujimoto, C. C. Dufort, M. A. Carlson, S. R. Hingorani, A. L. Paguirigan, J. P. Radich, D. T. Chiu, "Optical painting and fluorescence activated sorting of single adherent cells labelled with photoswitchable Pdots," *Nat. Commun.* **7**, 1–11 (2016).
41. D. Chen, I. C. Wu, Z. Liu, Y. Tang, H. Chen, J. Yu, C. Wu, D. T. Chiu, "Semiconducting polymer dots with bright narrow-band emission at 800 nm for biological applications," *Chem. Sci.* **8**, 3390–3398 (2017).
42. H. Park, K. Na, "Conjugation of the photosensitizer Chlorin e6 to pluronic F127 for enhanced cellular internalization for photodynamic therapy," *Biomaterials* **34**, 6992–7000 (2013).